Demonstration of Fully Integrated 6λ x 200 Gbps (1.2 Tbps) PICs and Transceivers in L-band

L. Chuang, L. Dardis, P. Abolghasem, A. Diba, M. Lu, T. Frost, B. Ellis, X. Xu, M. Montazeri, S. Murthy, A. Dentai, F. Sedgwick, M. Kuntz, J. Zhang, D. Pavinski, T. Butrie, S. DeMars, J. Rahn, V. Dominic, S. Corzine, V. Lal, P. Evans, M. Ziari, F. Kish

Infinera Corporation, 140 Caspian Court, Sunnyvale, CA 94089 (lchuang@infinera.com)

Abstract *We present the first fully monolithically integrated coherent receiver and transmitter PICs in L-band with performance capability comparable to their C-band counterparts, and demonstrate a C+L link with superchannels under dual-polarization, 16-QAM modulation at 33 GBaud (200 Gbps/λ).*

Introduction

L-band transmission has been increasingly considered as an alternative to scaling the fiber plant as it offers a nearly two-fold extension of fiber capacity. Link experiments have demonstrated record capacity for C+L band transmission enabled through an assembly of discrete optical components and powered by L-band tunable lasers[1]. There has been limited development of complete photonic integrated solutions to enable economic viability of L-band systems. Demonstrations to date have been limited to passive Si-photonics transmitter and receiver chips for coherent applications[2], 4 × 56 Gb/s EML array[3] or other single laser or detector devices. We report the first demonstration of fully monolithically integrated 6λ x 200 Gbps InP coherent transmitter and receiver PICs with fully tunable L-band lasers and present multi-span and multi-channel fiber link performance. This provides a two-fold fiber capacity expansion to our previously reported C-band counterpart[4-6].

Coherent L-band PIC architecture

The L-band transceiver module reported in this work is a 1.2Tb/s optical engine that consists of fully monolithically integrated 6λ coherent Tx and Rx PICs, both on InP substrates. An architectural schematic is shown in Fig. 1 for Tx and Rx PICs. Similar to C-band PICs[4-5], the Tx/Rx PIC transmits/receives orthogonal, dual polarizations (DPs) per λ to/from the fiber. Signals on either the Tx or Rx PIC have to be TE polarized to maximize the widely tunable laser (WTL) and photodiode (PD) efficiencies. Free space optics including collimation lenses couple light between the PICs and the fibers, and off-chip polarization beam combiners/splitters and polarization beam rotators mux/demux the orthogonal polarizations of a fiber into two TE polarized paths on a PIC, labelled TE and TE', respectively. On the Rx PIC, an incoming optical signal along the TE or TE' path is evenly divided and fed into 6 channels via power splitters. For a given channel, this amplitude- and phase-encoded signal is then combined with the output of a local oscillator (LO), which is a WTL, inside a 90-degree optical hybrid and is detected by an array of high-speed photodetector pairs.

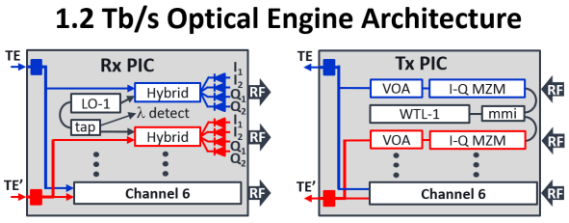

Fig. 1: 1.2 Tb/s optical engine architecture comprised of coherent L-band Rx and Tx PICs. There are two polarization inputs (outputs) labeled TE and TE' that are split (combined) on the Rx (Tx) PICs for the 6 channels.

Identical L-band WTLs are used on Rx PICs as LOs and on Tx PICs as DC signal sources before RF modulation. The WTL consists of a gain section, a phase-tuning section, and independently tunable, grating-based front- and back-mirrors with comb-like mirror reflectivity spectra. The two mirrors have different comb spacings designed with the Vernier effect to have a wider than 40 nm wavelength range in L-band that can be covered without any gaps. Inside the laser cavity, an independently tunable phase section aligns the cavity mode to the designed lasing wavelength. A power tap is added to the LO on the Rx PIC for laser characterization.

On the Tx PIC, the WTL for a given channel is split and fed into TE and TE' polarization paths. Each path consists of a nested I-Q Mach-Zehnder modulator (MZM) for amplitude and phase encoding which operates up to 33 Gbaud. To achieve 200 Gb/s per λ, DP 16-QAM modulation is used in this work. A variable optical attenuator (VOA) downstream of the MZM further balances the signal power between all the channels of the same polarization path (TE or TE'), then all channels are power-combined into a single output and routed to the facet.

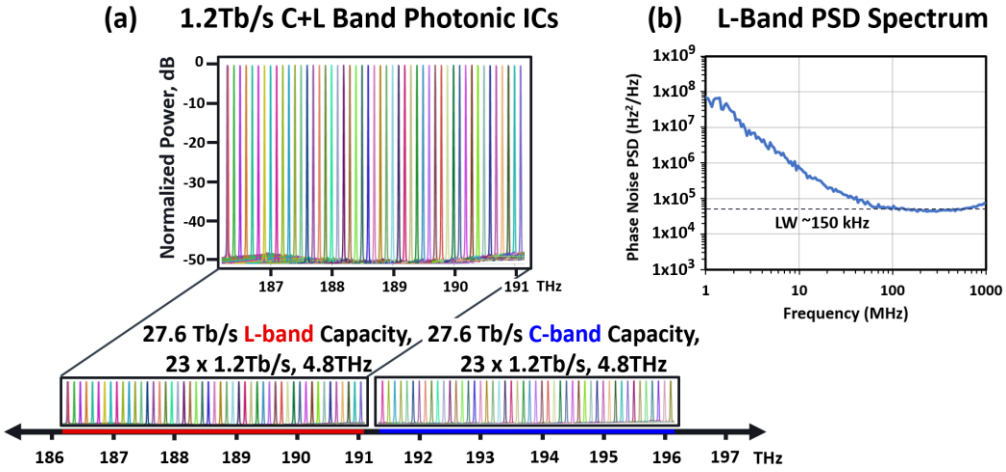

Fig. 2: (a) Transmitter normalized DC power vs. frequency for L-band or C-band PICs in steps of 100 GHz. 200 Gb/s per wave systems can achieve 27.6 Tb/s from each of C or L band for 55.2 Tb/s total from 276 waves and 46 modules for C+L bands. (b) Phase noise power spectral density (PSD) for a representative L-band WTL. The inferred linewidth is ~150 kHz.

Widely-Tunable Laser Performance

In this work, the L-band is defined as a 4.8 THz wide band from 186.250 THz to 191.050 THz (~40 nm), adjacent to and redder than the extended C-band (191.325 THz to 196.125 THz). We have previously reported on realization of 27.6 Tbps fiber capacity within the 4.8 THz bandwidth of C-band using near-Nyquist spectral efficiency superchannels[6]. The L-band WTLs were first characterized under CW operation. Fig. 2(a) shows the combined spectra from one L-band WTL and one C-band WTL. Normalized optical spectra with 100 GHz spacing is shown in this figure to demonstrate the full 4.8 THz L-band wavelength tunability with a single L-band WTL. Although the optical system demands a 4.8 THz coverage, the L-band WTL is tunable over at least 5.5 THz to provide design and manufacturing margin. The L-band side-mode suppression ratio (SMSR) is at least 48 dB, which is comparable to that of the C-band WTLs. The power required for the continuous L-band wavelength tuning is less than 120 mW per mirror. The required L-band gain current and phase-tuning power are at most 200 mA and 30 mW and are comparable to the C-band WTLs reported previously[4]. Fig 2(b) shows a representative FM spectrum for a Tx L-band WTL and was derived from a high-speed oscilloscope measurement with the RF circuit under modulation. The PSD phase noise is below $5x10^4$ Hz^2/Hz and an inferred linewidth[7] of ~150 kHz.

L-Band PIC Performance

The performance capability of the L-band PICs is comparable to that of their C-band counterparts. Fig. 3 shows the cumulative distributions of several key PIC parameters for over 90 channels for each kind of PIC (L- or C-band, Rx or Tx). Two important parameters for Rx PICs, the facet responsivity and the IQ imbalance, show very similar cumulative distributions between L and C-band PICs. The similarity implies that the PD responsivity, waveguide propagation loss and the insertion losses for the elements such as power splitters, hybrids and PDs are all comparable between L-band and C-band PICs.

The similarity in cumulative distribution can also be seen for the Tx parameters shown in Fig. 3. Similar WTL threshold current and the output power distributions testify to the optimization and uniformity of the L-band lasers. The similarity in the modulator V_{pi} further demonstrates that the

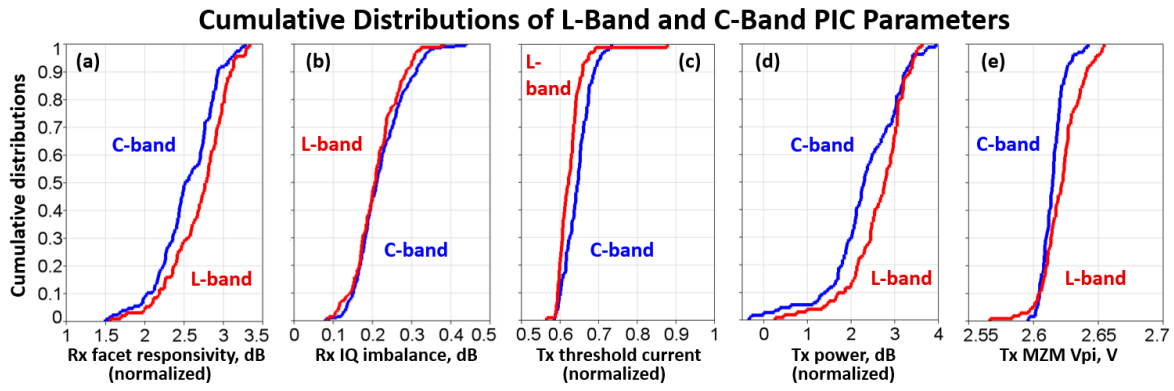

Fig. 3: Channel-level L-band and C-band cumulative distributions of key parameters over their entire respective bands. (a) Rx PIC facet responsivity normalized to spec at 0 dB, (b) IQ imbalance magnitude, (c) Tx PIC laser threshold current normalized to the spec (1x), (d) the Tx laser power normalized to spec at 0 dB, and (e) the Tx PIC MZM V_{pi} distribution.

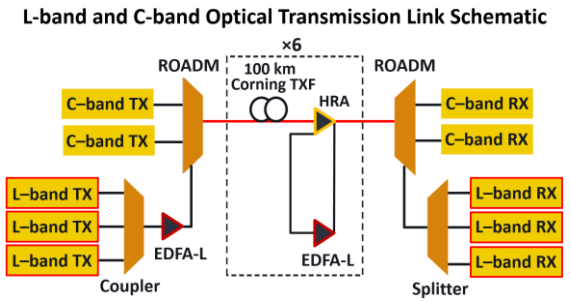

Fig. 4: Transmission testbed schematic

L-band MZMs have comparable performance to C-band PICs when correctly designed.

C+L System Performance

Fig. 4 shows the C+L band optical line system used as the testbed. The L-Band PICs are packaged and integrated onto the line cards with the DSP chips similar to Ref. 6 . The transmission demonstration includes two C-band and three L-band superchannels, each consisting of six 33 GBaud DP 16-QAM wavelengths, spaced by 37.5GHz. Adjacent superchannels are separated by a 12.5 GHz guard-band. The central frequencies of the five superchannels are 188.40, 188.65, 188.90, 193.70 and 193.95 THz. The three L-band superchannels are multiplexed with a coupler and then amplified by an L-band EDFA to reach a target power of -1 dBm/channel. The amplified L-band superchannels are combined with the C-band superchannels by a colored filter. The transmission link contains 6 spans of 100 km Corning TXF fiber™, each with approximately 17dB loss followed by a hybrid Raman amplifier (HRA) and an L-band EDFA. After transmission, the L-band superchannels are de-multiplexed from the C-band superchannels, and then broadcast to the L-band receivers.

The transmitted and received C+L band optical spectra are shown in Fig. 5. The L-band spectrum exhibits a slightly larger noise floor than the C-band because the C-band superchannels are multiplexed and filtered by a wavelength selective switch (WSS) while the L-band superchannels are power multiplexed, adding their unfiltered broadband ASE noise. After transmission through the system, the L-band superchannels achieve Q > 7.7dB and well above the forward error correction (FEC) threshold for error free operation. The transmission length is limited by the available number of spans used in this work, not by the transceiver modules. We expect further improvements of these L-band line cards with further optimization.

Conclusions

We demonstrated successful C+L band transmission and reception with DP 16-QAM modulation format at 33 GBaud over a 600 km

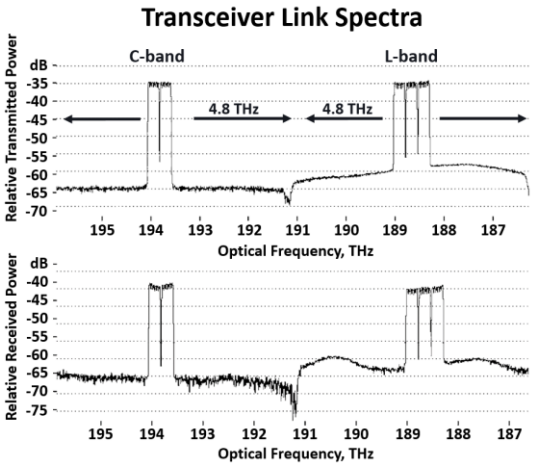

Fig. 5: Transmitted (top) and received (bottom) spectrum from 2×6 C-band channels and 3×6 L-band channels transmitted over a 600 km fiber link. The C-band channels benefit from WSS ASE filtering, but L-band channels do not. Optical systems that utilize both C- and L-bands access 9.6 THz of bandwidth.

reach. The L-band superchannel Q is greater than 7.7 dB and error free through FEC. The 600 km reach is merely limited by the available fiber spans in the test lab but not by the L-band transceivers themselves. These 6λ L-band Rx and Tx PICs deliver a post-FEC data rate of 200 Gbps per λ, and a 6λ transceiver capacity of 1.2 Tbps. These multi-channel L-band PICs, consisting of WTLs, PDs, hybrids, MMIs, MZMs, VOAs, all monolithically integrated on InP substrates, show similar performance capability compared to their C-band counterparts.

References

[1] A. Ghazisaeidi et al., "Advanced C+L-Band Transoceanic Transmission Systems Based on Probabilistically Shaped PDM-64QAM", J. Lightwave Technol., Vol. **35**, no. 7, p. 1291 (2017).

[2] C. Doerr et al., "O, E, S, C and L Band Silicon Photonics Coherent Modulator/Receiver", Proc. OFC, Th5C.4, Anaheim (2016).

[3] M. Theurer et al., "4 x 56 Gb/s High Output Power Electroabsorption Modulated Laser Array With up to 7 km Fiber Transmission in L-Band", J. Lightwave Technol., Vol. **36**, no. 2, p. 181 (2018).

[4] V. Lal et al., "Extended C-band Tunable Multi-Channel InP-Based Coherent Transmitter PICs", J. Lightwave Technol., Vol. **35**, no. 7, p. 1320 (2017).

[5] A. Hosseini et al., "Extended C-Band Tunable Multi-Channel InP-Based Coherent Receiver PICs", Opt. Express, Vol. **25**, no. 16, p. 18853 (2017).

[6] J. Rahn et al., "DSP-Enabled Frequency Locking for Near-Nyquist Spectral Efficiency Superchannels Utilizing Integrated Photonics", Proc. OFC, W1B.3, San Diego (2018).

[7] K. Kikuchi, "Effect of 1/f-Type FM Noise on Semiconductor-Laser Linewidth Residual in High-Power Limit", IEEE J. Quantum Electron., Vol. **25**, no. 4, p. 684 (1989).